erase in mammalian liver. Of interest in this regard is the recent report by Scrutton *et al.* (*13*) that RNA polymerase of *E. coli* is a zinc metalloenzyme. Our findings complement this report. Taken together, these two reports may help solve part of the puzzle of the role of zinc in the metabolism of RNA.

M. W. TERHUNE
H. H. SANDSTEAD*
Division of Nutrition, Vanderbilt University School of Medicine, Nashville, Tennessee 37203

References and Notes

1. M. Fujioka and I. Lieberman, *J. Biol. Chem.* **239**, 1164 (1964).
2. R. B. Williams, C. F. Mills, J. Quartman, A. C. Dalgarno, *Biochem. J.* **95**, 290 (1965).
3. H. H. Sandstead and R. A. Rinaldi, *J. Cell. Physiol.* **73**, 81 (1969).
4. R. C. Theuer and W. G. Hoekstra, *J. Nutr.* **89**, 448 (1966); J. M. Hsu, W. L. Anthony, R. J. Buchanan, *ibid.* **99**, 425 (1969); J. M. Hsu and W. L. Anthony, *ibid.* **100**, 1189 (1970).
5. D. Mikac-Devic, *Advan. Clin. Chem.* **13**, 271 (1970).
6. L. M. S. Chang and F. J. Bollum, *Proc. Nat. Acad. Sci. U.S.A.* **65**, 1041 (1970); J. P. Slater, A. S. Mildvan, L. A. Loeb, *Biochem. Biophys. Res. Commun.* **44**, 37 (1971).
7. W. E. C. Wacker and B. L. Vallee, *J. Biol. Chem.* **234**, 3257 (1959); H. Altmann, F. Fetter, K. Kaindl, *Z. Naturforsch.* **234**, 395 (1968); Y. A. Shin and G. L. Eichorn, *Biochemistry* **7**, 1026 (1968); M. Tal, *Biochem. Biophys. Acta* **195**, 76 (1969).
8. H. H. Sandstead and M. W. Terhune, in *Clinical Applications of Zinc Metabolism*, W. Pories and W. Strain, Eds. (Thomas, Springfield, Ill., in press).
9. P. B. Mutch and L. S. Hurley, *Fed. Proc.* **30**, 2501 (1971).
10. C. C. Widell and J. R. Tata, *Biochem. J.* **92**, 313 (1964).
11. S. B. Weiss, *Proc. Nat. Acad. Sci. U.S.A.* **46**, 1020 (1960).
12. K. W. Giles and M. A. Meyers, *Nature* **206**, 93 (1965).
13. M. C. Scrutton, C. W. Wu, D. A. Goldwait, *Proc. Nat. Acad. Sci. U.S.A.* **68**, 2497 (1971).
14. Supported by a Future Leaders grant from the Nutrition Foundation to H.H.S. and an NSF fellowship to M.W.T.
* Present address: Human Nutrition Laboratory, U.S. Department of Agriculture, Grand Forks, N.D. 58201.

4 February 1972; revised 4 April 1972

Antidromic Action Potentials Fail to Demonstrate Known Interactions between Neurons

Abstract. *An identified motor neuron in the stomatogastric ganglion of* Panulirus interruptus *inhibits four other motor neurons when it fires spontaneously or in response to depolarization of its soma. It does not inhibit these neurons when it is fired antidromically, although the attenuated antidromic spike is visible at its soma. These findings point out the difficulty of interpreting negative results from antidromic stimulation experiments and the importance of neuronal structure to the integrative activities of nervous systems.*

Antidromic action potentials are action potentials that start at some unusual site on an axon and travel back toward the normal site of initiation. In the laboratory, such potentials commonly arise because an experimenter stimulates the axon electrically, trying to get such a potential to invade the integrative regions of the neuron. One reason for doing so is to look for interactions between the neuron stimulated and other neurons being monitored during the stimulation [for example, see (*1*)]. The assumption one would like to make is that antidromic potentials will behave in the neuron as do orthodromic potentials, those which arise at the usual initiation site and travel in the usual direction down the axon. According to this assumption, if antidromic potentials reveal interactions between neurons, these interactions also occur when orthodromic spikes arise, and if antidromic potentials do not reveal interactions between neurons, these interactions do not occur when orthodromic spikes arise. This report shows that, in one case, the assumption does not hold, and so challenges its validity in general.

The stomatogastric ganglion of the spiny lobster, *Panulirus interruptus*, has 30 to 36 neurons; it lies on the dorsal side of the stomach in the lumen of the dorsal aorta and controls the numerous striated muscles that move different sections of the stomach. These neurons are monopolar; each neuronal soma is connected to the integrative regions of the neuron by a neurite that does not support a conducted action potential. The spike-initiating zone, the axon, and the branches that form synapses with other neurons are all removed from the soma. The ganglion is an ideal system for testing the logic of antidromic stimulation, since we can regularly record subthreshold synaptic activity as well as attenuated action potentials from the somata of identified neurons, and simultaneously record the action potentials of these neurons in the peripheral nerves. Careful dissection produces a preparation in which the axons of many neurons are separately accessible and can be used for both recording and antidromic stimulation. Using this system, we have shown that inhibitory postsynaptic potentials (IPSP's), which always occur in four identified cells when a particular fifth cell fires spontaneously or in response to depolarization of its soma, do not occur when the fifth cell is invaded by an antidromic action potential originating outside the ganglion.

The stomatogastric ganglion and its associated nerves were dissected free of the stomach. Each nerve was identified by its route from the ganglion to the muscles that it innervated, by use of the anatomic description by Dando and Maynard (*2*). The isolated ganglion and nerves were then pinned out in a Sylgard-lined petri dish. The ganglion was desheathed and transilluminated. The preparation was maintained during dissection and subsequent experimentation in a saline solution containing 521 m*M* Na^+, 10 m*M* K^+, 16.7 m*M* Mg^{2+}, 16.7 m*M* Ca^{2+}, 21 m*M* SO_4^{2-}, 557 m*M* Cl^-, and 3 m*M* *N*-tris(hydroxymethyl)methyl-2-aminoethane sulfonic acid. The *p*H was adjusted to 7.3 to 7.5 with NaOH. The saline was aerated overnight before use, and 2 m*M* glucose was added at the start of the experiment. During the dissection, the saline was cooled to about 10°C. The experiments were performed at room temperature, 20°C.

Action potentials were recorded from the nerves with 100-μm stainless steel electrodes pinned into the Sylgard in a monopolar configuration (*3*). The potentials were differentially amplified, displayed on an oscilloscope, and recorded on a frequency-modulated tape recorder for subsequent filming. The recording electrodes could also be used for antidromic stimulation; a simple switching network allowed us to change the function of the electrode without disturbing the preparation. The stimuli were isolated from ground.

Intracellular recordings were made by desheathing the ganglion and then penetrating the somata of particular cells with glass capillary microelectrodes filled with 2.5*M* KCl. Electrode resistances varied from 20 to 50 megohms. The intracellular potentials were observed through a W-P Instruments M4A preamplifier, displayed on an oscilloscope, and recorded on a frequency-modulated tape recorder. The membrane potentials of the cell could be controlled by passing current through the microelectrode by means of the current-injection feature of the preamplifier.

The isolated stomatogastric ganglion

produces two separate rhythms of activity in different sets of motor neurons. One of these sets—the pyloric system—contains 14 neurons and is characterized by periodic bursts of action potentials in a group of three neurons—the two pyloric dilator (PD) neurons and the anterior burster (AB) neuron (*4*). The axons of the PD neurons run in the ventral lateral ventricular nerve (v-LVN), while the axon of the AB neuron runs in the stomatogastric nerve. The PD and AB neurons are tightly coupled electrotonically and receive very similar synaptic input (*5*). Since recordings from any of these cells give results that are identical as far as this discussion is concerned, we consider the cells as equivalent here.

Another cell in the pyloric system, the lateral pyloric (LP) neuron, inhibits the PD and AB neurons when it fires and is inhibited when the PD and AB neurons fire (*4*). Figure 1a is a film of several cycles of the pyloric rhythm, showing the periodicity of the PD burst, the inhibition of the LP neuron, and the reciprocal inhibition of the PD cell. The LP spikes produce large IPSP's in the PD cell. The axons of both the PD and the LP cells run through the v-LVN before reaching the muscles they innervate, and so the spikes of both neurons can be recorded in the v-LVN and differentiated by amplitude. The LP neuron also inhibits another element of the pyloric system, the ventricular dilator (VD) neuron, whose axon runs in the median ventricular nerve (MVN). Figure 1b is a film of several cycles of the pyloric rhythm in another preparation, showing spontaneous activity in the VD and LP neurons. When the VD neuron fires, it does not affect either the LP neuron or the PD and AB neurons. When the LP neuron fires, it causes an IPSP in the VD neuron. Both the VD and LP neurons are inhibited by the PD and AB neurons (*4*). The PD spikes can be seen on the v-LVN trace, but the correlation of the PD spikes and the IPSP's in the VD and LP is obscured at these film speeds because the neurons of the PD and AB group do not fire synchronously, and the IPSP's from each are imperfectly superimposed. These interactions between the LP, VD, and PD neurons are summarized in Fig. 1c.

When the soma of the LP neuron is depolarized, the cell will fire. Figure 2a is a film of such a depolarization in the same preparation as used for Fig. 1b. The resulting spikes are visible on the v-LVN trace. The spikes correlate one-to-one with IPSP's that appear on the PD and VD traces during the depolarization. This shows that, as far as these two synapses are concerned, spikes arising spontaneously and spikes arising in response to depolarization of the soma are equivalent. In the experiment illustrated in Fig. 2, the spikes in the PD trace were not as large as usual. During the depolarization of LP, the LP trace moved above the VD trace, where the resulting spikes can be seen just below the PD trace. At the end of the depolarization, it fell back into place below the VD trace.

When an antidromic action potential invades the LP neuron, no IPSP's occur in the VD or PD neurons. Nevertheless, the antidromic spike is visible in the soma as an attenuated spike of nearly the same size as spikes that occur spontaneously. In the experiment filmed in Fig. 2b, the LP axon was isolated after it left the v-LVN. Therefore, we could stimulate it alone and record both ortho- and antidromic LP spikes in the v-LVN. At the start of the upper record of Fig. 2b, a stimulus train to the LP axon began at 2 hertz. At the upward arrow, the stimulus intensity was increased slightly, and an antidromic spike was recruited in the LP neuron (Fig. 2, c and d). This spike was recorded both at the v-LVN electrode and in the soma, but no IPSP appeared in either the VD or PD neurons. The failure of the antidromic spike to reach the synapses was not frequency-dependent in the range 2 to 10 hertz. At the downward arrow in Fig. 2b, the stimulus intensity was reduced below threshold, but the disappearance of the antidromic LP spikes did not affect the VD or PD neurons.

Perhaps the clearest proof of the difference between orthodromic and anti-

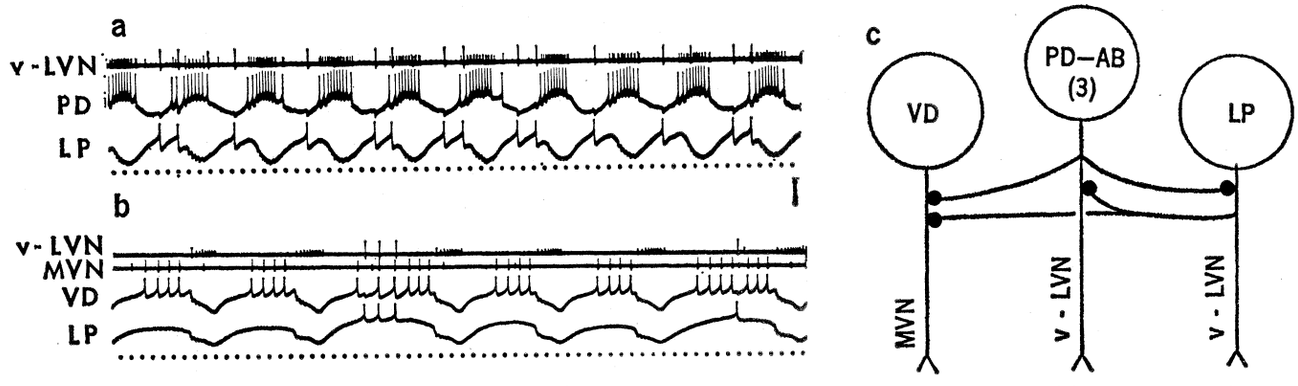

Fig. 1. (a) Spontaneous activity in one of the two pyloric dilator (PD) neurons and the lateral pyloric (LP) neuron of an isolated stomatogastric ganglion from *Panulirus interruptus*. The action potentials in each neuron were recorded both in the ventral lateral ventricular nerve (v-LVN) and as attenuated spikes in the soma of the neuron. The intracellular records show the action potentials superimposed on the slow oscillations of membrane voltage characteristic of these cells. Each action potential in the PD neuron causes a small inhibitory postsynaptic potential (IPSP) in the LP neuron, and these IPSP's seem to depress the membrane voltage of the LP neuron during the PD burst. Each action potential in the LP cell causes a large IPSP in the PD neuron. The LP spikes on v-LVN were retouched. The time marker (dots) shows 100-msec intervals. The voltage calibration (vertical line) is 20 mv. (b) Spontaneous activity in a ventricular dilator (VD) neuron and an LP neuron. The action potentials in each neuron were recorded both as attenuated spikes in the soma and at a point on the peripheral nerves where its axon ran. The VD action potentials were recorded in the median ventricular nerve (MVN) and the LP action potentials in the v-LVN. The v-LVN trace also shows the action potentials of the PD neurons, which inhibit both the VD and LP neurons. Each action potential in the LP neuron causes an IPSP in the VD neuron, two of which occur on the falling phase of VD spikes and so are obscured. However, they delay the next VD spike. Time marker, 100-msec intervals; voltage calibration, 20 mv. (c) A summary diagram of the intracellular connections that generate the synaptic effects described above. The three neurons of the PD-AB group inhibit both the VD and LP neurons. The LP neuron inhibits the PD, AB, and VD neurons. The actual locations of these synapses on each cell are not known.

dromic spikes in the LP neuron is their effect on the pyloric rhythm as a whole. When the LP neuron fires spontaneously, the PD burst is delayed (Fig. 1). Similarly, the spikes that resulted from depolarizing the LP soma (Fig. 2a) delayed the next PD burst. But the antidromic spikes affected neither the frequency of bursts in the PD unit, nor the number of spikes per burst in the VD neuron. This is the sort of evidence that would normally be taken as evidence for the absence of interaction between neurons, if no subthreshold data were available.

Why do the antidromic action potentials fail to reach the inhibitory synapses? A comparison of the shapes of ortho- and antidromic spikes offers a clue. The spontaneous orthodromic spikes (Fig. 1b) rise from a slower depolarization reminiscent of a generator potential. The spikes caused by depolarization of the soma (Fig. 2a) show a similar slow rise, but the antidromic spikes (Fig. 2b) rise abruptly. The current flow associated with a spontaneous action potential or caused by somatic depolarization appears to be greater than that associated with an antidromic spike. This graded current may contribute to the ability of orthodromic spikes to reach the synapses. Alternatively, if the antidromic spikes are blocking at some point distal to the normal spike-initiating zone, their failure to reach the synapses in question may be due to this factor alone. A spike started at the normal point might propagate down more than one process of the neuron. Since the shape and amplitude of the attenuated spontaneous spikes recorded in the soma are the same as those of spikes caused by depolarization of the soma, it seems likely that they are initiated at the same point. But antidromic spikes might never reach cell processes other than the axon because they block before they get to these processes. The slightly larger amplitude of orthodromic spikes recorded in the soma indicates that the point at which they fail is slightly closer to the soma than that at which the antidromic spikes fail (*6*).

Studies of frequency-dependent blocking of spikes at branch points in sensory afferents entering the spinal cord of frogs and in motor neurons innervating two muscles in the crayfish abdomen (*7*) suggest that the structure of neurons can influence their ability to handle signals. In the limited range of frequencies examined, we saw no evidence of frequency sensitivity of the antidromic spike blockade in the LP neuron, but it seems probable that the structural factors which cause the antidromic spikes to block in the LP are similar to those which caused the blockage in the frog sensory afferent and in the crayfish motor axon.

The interpretation of negative results from antidromic stimulation experiments has always been a difficult

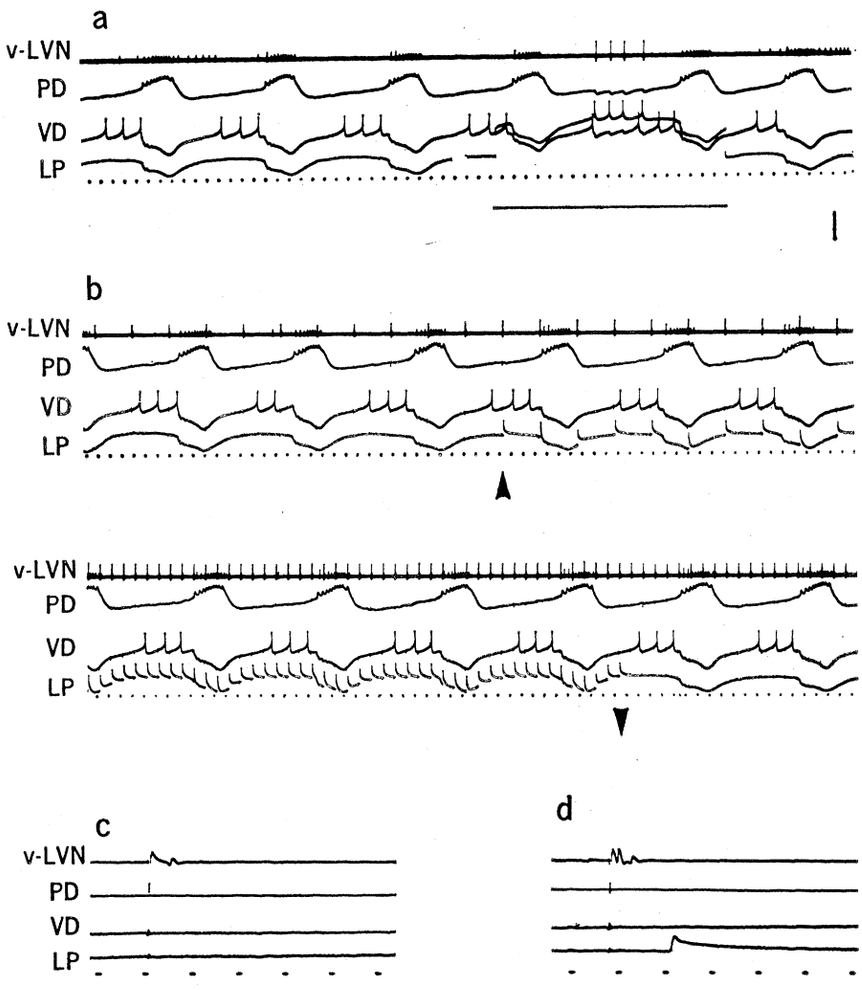

Fig. 2. (a) Depolarization of the LP neuron at its soma causes the cell to fire and inhibit both the PD and VD neurons. During the period marked by the solid bar, the LP neuron was depolarized. Its action potentials are visible on the v-LVN trace and as attenuated spikes on the intracellular trace displaced above the VD trace. Both the PD and VD traces show IPSP's at a constant latency following each LP action potential. At the beginning and end of the v-LVN trace, there are additional spikes with amplitudes similar to those of the PD spikes. These are from an identified unit that is not part of the pyloric system. Time marker (dots), 100-msec intervals; voltage calibration (vertical line) for LP and VD, 20 mv; for PD, 25 mv. (b) Antidromic action potentials in the LP neuron are visible in the soma as attenuated spikes of approximately the same amplitude as orthodromic spikes. They do not inhibit either the PD or the VD neurons. The stimuli were applied to the lateral pyloric nerve distal to the v-LVN and monitored on the v-LVN. They began at about 2 hertz and were increased slowly to 10 hertz. At the upward arrow, the intensity of the stimulation was increased, recruiting an antidromic spike in the LP neuron. This and subsequent spikes did not cause IPSP's in the VD or PD neurons. No change in the response occurred as the stimulus intensity was decreased below threshold again, although the stimulus train continued. The cessation of LP action potentials did not affect either the PD or VD neurons. The two sections are not continuous. Figures 1b and 2, a to d, are from the same experiment. Time marker, 100-msec intervals; voltage calibration, same as in Fig. 2a. (c) A high-speed photograph of the stimulus preceding the one marked by the upward arrow in Fig. 2b. No response occurs in the LP neuron. Time marker, 10-msec intervals; voltage calibration, same as in Fig. 2a. (d) A high-speed photograph of the stimulus marked by the upward arrow in Fig. 2b. An additional spike appears approximately 2 msec after the stimulus on the v-LVN trace, and a spike appears in LP trace about 10 msec later. These two events showed a sharp threshold, all-or-nothing behavior and always occurred together. Time marker, 10-msec intervals; voltage calibration, same as in Fig. 2a.

business. We think that the results presented here force a more rigid interpretation of such experiments. Positive results, those which demonstrate interactions between cells, can safely be taken at face value; negative results are not interpretable because they fail to distinguish between the alternate possibilities that interactions do not exist or that antidromic spikes do not reach the site of interaction.

BRIAN MULLONEY
ALLEN SELVERSTON
Department of Biology,
University of California, San Diego,
La Jolla 92037

References and Notes

1. B. Mulloney, *J. Neurophysiol.* **33**, 86 (1970).
2. M. Dando and D. M. Maynard, in preparation.
3. K. G. Pearson, R. B. Stein, S. K. Malhotra, *J. Exp. Biol.* **53**, 299 (1970).
4. D. M. Maynard, *Ann. N.Y. Acad. Sci.*, in press.
5. B. Mulloney and A. Selverston, in preparation.
6. L. Tauc and G. M. Hughes, *J. Gen. Physiol.* **46**, 533 (1963), thoughtfully reviewed by D. Kennedy, *Advan. Comp. Physiol. Biochem.* **2**, 117 (1966).
7. S.-H. Chung, S. Raymond, J. Y. Lettvin, *Brain Behav. Evol.* **3**, 72 (1970); I. Parnas, *Biol. Bull.* **139**, 432 (1970).
8. We thank Donald Kennedy for the original suggestion that we check the effectiveness of antidromic spikes in these cells. Supported by an NIH postdoctoral fellowship to B.M. and by NIH grant NS 09322-02 to A.S.

21 December 1971; revised 13 March 1972

Chromosomal RNA: Its Properties

Abstract. *We describe the properties of a special class of RNA associated with chromatin. We discuss why this RNA should be considered a distinct class of RNA and not an artifactual degradation product of either transfer or ribosomal RNA.*

We have described the preparation and properties of a class of RNA molecules associated with chromosomes, which we have termed chromosomal RNA or cRNA (*1–3*). It has been suggested that cRNA may be an artifact resulting from the degradation of transfer RNA (tRNA) (*4*), or that it may not exist at all (*5*, *6*). In this report we describe the known properties of cRNA and show that cRNA from Novikoff ascites in the rat is not detectably contaminated with tRNA, ribosomal RNA (rRNA), or their degradation products. We review the methods available for the isolation of cRNA and discuss whether cRNA should be considered a distinct class of RNA.

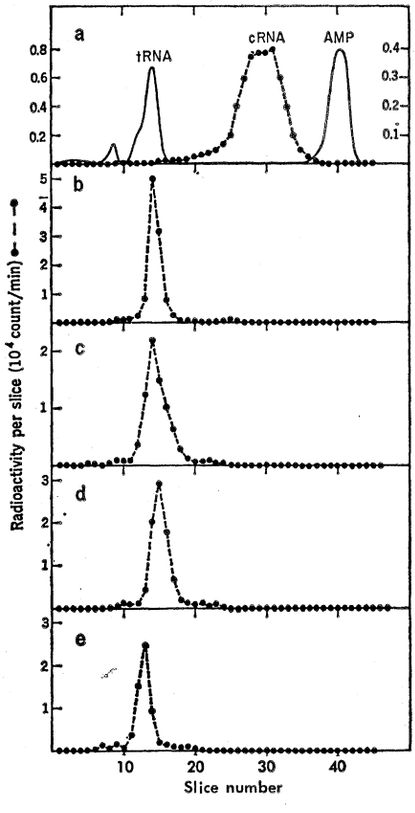

Fig. 1. Separation of tRNA, cRNA, and adenosine monophosphate (AMP) by polyacrylamide gel electrophoresis. Samples were applied in 20 μl of 50 percent glycerol (by volume) to a 6-cm column containing 14 percent acrylamide and 0.1 percent sodium dodecyl sulfate, and 5 ma per gel was applied for 2.5 hours. (a) The sample was [^{3}H]cRNA prepared from rat Novikoff ascites by a method similar to that of Dahmus and McConnell (*3*), yeast tRNA (Sigma), and AMP. Absorbance at 260 nm (scale at right) is given by the solid line. (b) The sample, [^{3}H]tRNA prepared from rat Novikoff ascites as described by Dahmus and McConnell (*3*) and stored at −18°C in 1 m*M* ethylenediaminetetraacetic acid, was applied directly to the gel without prior treatment. (c) The [^{3}H]tRNA in (b) was incubated in 0.01*M* tris(hydroxymethyl)-aminomethane (tris), *p*H 8, at 37°C for 2 hours before electrophoresis. (d) The preparation in (b) was incubated in 0.01*M* tris, *p*H 8, plus Pronase B (Calbiochem), 2 mg/ml, at 37°C for 2 hours before electrophoresis. The Pronase had been first incubated in 0.01*M* tris, *p*H 8, for 90 minutes at 37°C at a concentration of 20 mg/ml. (e) The sample was prepared as in (d) except that Pronase C (Calbiochem), 2 mg/ml, was used in place of Pronase B. The Pronase was first incubated as described in (d).

Three principal properties identify cRNA. First, it elutes as a symmetrical peak from diethylaminoethyl (DEAE) Sephadex in 7*M* urea at approximately 0.55*M* NaCl (*2*, *3*, *7–13*) and from DEAE cellulose at 0.38*M* NaCl (*11*, *14*, *15*). Second, cRNA hybridizes to DNA to a much larger extent than does either tRNA or rRNA (*2*, *3*, *8*, *14*). We have yet to isolate cRNA from any tissue which hybridizes to less than 2 percent of homologous DNA (*2*, *3*, *8–11*, *16*). Further, cRNA from pea buds (*7*) and rat ascites (*8*) hybridizes to the middle-repetitive sequences of homologous DNA. Third, cRNA isolated from a wide variety of organs and organisms contains from 7 to 10 percent dihydropyrimidine (*3*, *8–12*, *15*, *19*, *20*).

Both cRNA and tRNA elute from DEAE Sephadex at 0.55*M* NaCl in 7*M* urea. The contamination of cRNA by tRNA is minimized by using isolated chromatin as the starting material. Even if purified tRNA or isolated ribosomal subunits are added to isolated chromatin and the chromatin is processed for cRNA by the method of Dahmus and McConnell (*3*), less than 1 percent of the cRNA peak recovered on DEAE Sephadex is either tRNA or rRNA (*21*). The following observations also demonstrate that cRNA is not related to either tRNA or rRNA.

1) Ascites cRNA can be separated from tRNA on DEAE cellulose (*11*, *14*, *15*), Sephadex G100 (*8*), or by disc gel electrophoresis (Fig. 1a).

2) If tRNA is subjected to the same Pronase treatment that is used in the isolation of cRNA, no degradation of tRNA to fragments the size of cRNA is detected (Fig. 1, b to e). This result is not in agreement with one report (*4*). The discrepancy is probably due to the quality of Pronase used, that is, to residual ribonuclease activity present in those Pronase samples which do degrade tRNA.

3) Ascites cRNA hybridizes to an estimated 4.9 percent of rat DNA, whereas tRNA hybridizes to about 0.09 percent of rat DNA under the same conditions (Fig. 2, a and b). The relation between base sequences of ascites cRNA and tRNA has been tested by reciprocal competition experiments. At the level of sensitivity of these experiments, no relation could be found between these base sequences (Table 1). Furthermore, cRNA hybridizes exclusively to purified middle-repetitive DNA (*8*) and in a DNA-driven RNA hybridization reaction has a $Cot_{1/2}$